

On the Second Explosion Limits of Hydrogen, Methane, Ethane, and Propane

Jie Liu,* Ruiguang Yu, Biao Ma, and Chenglong Tang*




Cite This: *ACS Omega* 2020, 5, 19268–19276



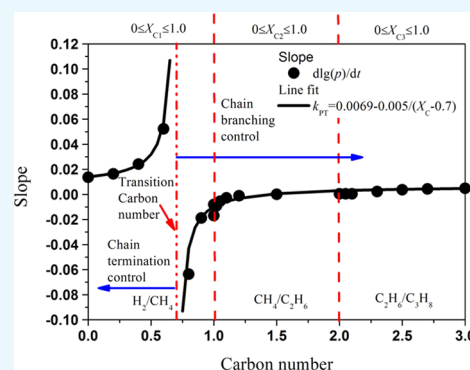
Read Online

ACCESS |

 Metrics & More

 Article Recommendations

ABSTRACT: In this work, we have first investigated the explosion limit behaviors from hydrogen to propane through numerical simulations and validated with the available experimental data. The shape of the explosion limit curves and the possible turning points (P_{1-2} , T_{1-2}), first to second limit transition, and (P_{2-3} , T_{2-3}), second to third limit transition that bound the second explosion limit as a function of the fuel carbon number, have been examined. Results show that with an increase of methane mole fraction in the hydrogen/methane system, the upper turning point (P_{1-2} , T_{1-2}) remains almost unchanged and the lower transition point (P_{2-3} , T_{2-3}) rotates counterclockwise around (P_{1-2} , T_{1-2}). With a further increase of carbon number, (P_{1-2} , T_{1-2}) moves to the lower-pressure and -temperature region and (P_{2-3} , T_{2-3}) gradually moves to the lower-pressure and higher-temperature region. The slope of the second explosion limit is inversely proportional to the carbon number, $k_{PT} = 0.0069 - 0.005/(X_c - 0.7)$, approximately. Second, a sensitivity analysis has been conducted to study the elementary reaction on the second explosion limits. The results show that the chain branching and termination reactions governing the explosion limit of hydrogen have a little effect on the second explosion limit of methane. The $C_2H_5O_2H$ decomposition to form OH radicals is dominant in controlling the nonmonotonic behavior of the second explosion limit of C_2H_6 . The second explosion limit behavior of propane is governed by three sets of reactions in the low-temperature oxidation process.



1. INTRODUCTION

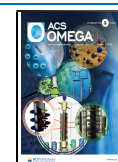
Flammable gases widely exist in petroleum, coal, chemical, metallurgy, textile, medicine, and other industries. Under certain conditions, the combustible mixture will explode in the processes of transportation, storage, mining, and utilization, resulting in a huge loss of life and property. Therefore, the phenomenon of explosion has always been concerned by researchers owing to the explosion characteristics,¹ minimum ignition energy,² and flammability characteristics.³ The explosion limits of a homogeneous fuel/oxidizer mixture that separates the explosive and nonexplosive regions are dominated by the competition of the radical producing and removing reactions, the result of which is pressure- and temperature-dependent.⁴ As such, the explosion limit is typically characterized in the pressure–temperature parameter space and can be described by the pressure as a complex function of the system temperature. As a prominent example, the explosion limit of the H_2 – O_2 mixture presents a Z-shaped curve, which consists of two turning points. The nonexplosion to explosion transition boundary divides the pressure vs temperature curve into the first, second, and third explosion limits under the low-, medium-, and high-pressure conditions, respectively.⁵ The first and third explosion limits are controlled by the competitive mechanism of the chain branching reactions and the diffusion mechanism of active radicals to

the wall (chain termination step), while the second limit relies primarily on the competition between chain termination and branching reactions.⁴ Semenov et al. studied the first explosion limit and found that the elimination of H radicals is more important than that of O and OH radicals when determining this limit.⁶ However, Glassman pointed out that at low pressures, the elimination of OH and H radicals was equally critical to the first explosion limit.⁷ When the pressure is sufficiently high, the reaction between HO_2 and H_2 produces H_2O_2 , which subsequently decomposes to two OH radicals and increases system reactivity. When this lumped channel overtakes the wall destruction mechanism of HO_2 , explosion happens again, and this critical pressure is the so-called third explosion limit.⁸ Recently, Sánchez observed that the third explosion limit can be well predicted by five HO_2 - and H_2O_2 -involving reactions.⁹

Received: June 14, 2020

Accepted: July 14, 2020

Published: July 24, 2020



The second explosion limit presents a significantly different characteristic compared with the first and third explosion limits. The appearance of the second explosion limit makes the explosion limit curve change from monotonic to non-monotonic.¹⁰ In particular, the second explosion limit of hydrogen is peculiar in that as the pressure is further increased inside the peninsular of the explosion regime, the mixture becomes nonexplosive. The second limit is the control limit of purified chemical kinetics, i.e., the free radical formation reaction competes with the termination reaction of the free radicals.¹¹ Moreover, as the three-body termination reaction $H + O_2 + M = HO_2 + M$ is pressure-sensitive, it will override the most effective chain branching reaction to generate the second explosion limit when the H_2/O_2 system moves from a lower pressure to a higher pressure under a constant temperature. The appearance of the second explosion limit of hydrogen then demonstrates that the reactivity of the system in the medium-pressure region is reduced.

Plenty of studies on H_2/O_2 systems have clearly recognized the three explosion limits and the corresponding controlling mechanisms for each limit. For explosion limits of larger molecules, however, only limited investigations have been conducted. Specifically, Liang et al. have investigated the hydrogen addition effect on the explosion limits of CO/O_2 mixtures and showed that the explosion curve changed from a C-shape to Z-shape with minute quantities of hydrogen addition, and the most severe change appeared in the second explosion limit region.¹² Subsequently, they investigated the CH_4/O_2 system and showed that the addition of 5% of H_2 also changed the monotonic explosion curve to the nonmonotonic Z-shaped one.¹³ The presence of inert gas in the system did not affect the shape of the explosion limit curve but only shifted the explosion limit curve to higher temperatures.¹⁴ Because propane occupies the position between lower and higher hydrocarbons, at very early times, Newitt and Thornes¹⁵ experimentally measured the ignition temperature of propane/oxygen in a closed homogeneous reactor with varying pressures. They showed that at lower and higher pressures, the ignition temperature decreased with increasing pressure, while at intermediate pressures, the ignition temperature increased with increasing pressure, which was consistent with the widely recognized negative temperature coefficient (NTC) behavior caused by the formation of cool flame. At the same time, low-temperature combustion is accompanied by a cool flame, which not only affects the safety of the engine but also plays an important role in the combustion technology of the advanced engine.¹⁶ Furthermore, the typical negative temperature coefficient (NTC) behavior was reported for larger alkanes.¹⁷ Recently, Yu et al. first investigated the effect of equivalence ratio and N_2 addition on the explosion limit of propane.¹⁸ After that, Liu et al. investigated the effect of O_3 addition on the cool flame region of the explosion limit of propane.¹⁹

The objectives of the present work are the following. Because only Newitt and Thornes reported the experimentally measured explosion temperature as a function of system pressure though that was decades ago and only propane was investigated. As such, our first objective is to use several well-recognized kinetic mechanisms that have been widely used in the combustion chemistry community to numerically investigate the explosion limit behaviors from hydrogen to propane with gradually increasing the carbon number in the system. The shape of the explosion limit curve and the possible turning

point shift as a function of the fuel carbon number will be examined. We note that the classic Z-shaped explosion limit curve has been widely recognized for the hydrogen/oxygen system, while fewer investigations for larger molecules have been reported. We also note that the second explosion limit depends on the competition between the chain branching and termination reactions, which may be complex and demands more investigations. As such, we will emphasize on the second explosion limit. Second, because the detailed mechanisms contain hundreds of chain branching and termination reactions, a sensitivity analysis will be conducted to find out the most important elementary reactions that control the second explosion limits of all of the C0–C3 alkane/oxygen systems. This can be realized by tuning the rate constant of each elementary reaction and accessing the response of the explosion limit curve, and by doing this, the sensitive reactions that affect the second explosion limit behaviors will be selected. These sensitive reactions will be subsequently removed individually from the mechanism, and the predictions from the mechanism without including these reactions will be compared with the original one to identify the controlling elementary reactions for the second explosion limit behaviors. In the following, we will specify our numerical method and the criterion of the explosion limit. Then, we will show our numerically calculated explosion limit curves using the validated kinetic mechanisms, followed by the effect of the dominant elementary reactions on the nonmonotonic second explosion limit curves.

2. NUMERICAL APPROACH METHOD

The explosion limits of C0–C3 alkanes are calculated using the SENKIN code.²⁰ An explosion is identified if the system temperature increases by 50 K compared with the initial temperature within 10 s under certain pressure conditions, as recommended in ref 5. The initial calculated pressure is ranged from 3.5 to 3.2×10^7 Pa, which covers the working range of the common combustion devices, and the explosion temperature searching range is 350–2500 K. Other criteria like an average pressure increase rate of 3%/ms can be found for the determination of the cool flame ignition.²¹

Three different detailed chemical kinetic models are used in this study, which are the comprehensive *iso*-octane combustion model (KAUST),²² Aramco 2.0 model,²³ and methane/propane oxidation model²⁴ from the National University of Ireland Galway (NUIG). As the KAUST and Aramco 2.0 models include larger hydrocarbon molecules, only the C3 subset species and related reactions are used in this study. Diffusion of the carriers to the chamber wall is assumed to be much faster than wall absorption since only a small amount of the carriers that reach the wall are absorbed.⁵ Moreover, concentrations of the carriers at the wall are assumed to be the same as those in the gas phase such that a zero-dimensional reactive system with a volume V and surface area S is assured.

The carriers are destroyed at the wall according to the reactions,

$H, O, OH, HO_2, H_2O_2, HCO \xrightarrow{k_H, k_O, k_{OH}, k_{HO_2}, k_{H_2O_2}, k_{HCO}} \text{wall}$
destruction, with the corresponding reaction rate per unit volume $k_H, k_O, k_{OH}, k_{HO_2}, k_{H_2O_2}$, and k_{HCO} given by

$$k = \frac{1}{2} \varepsilon \bar{v} \frac{S}{V} \quad (1)$$

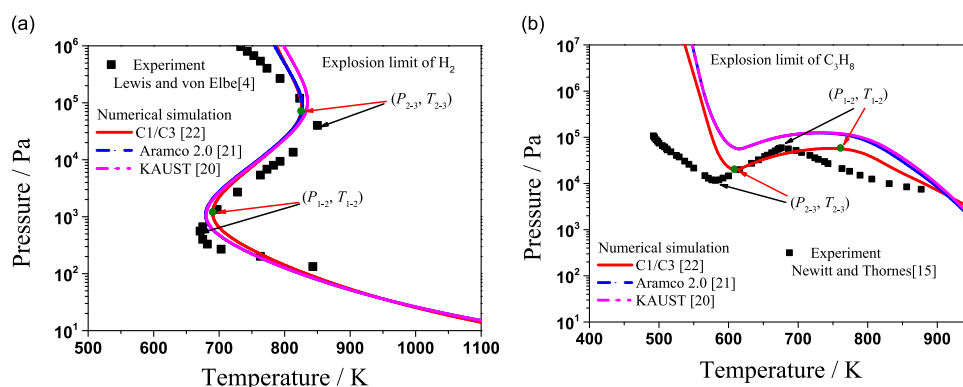


Figure 1. Comparison of the calculation and experimental explosion limits of hydrogen (a) and propane (b); the experiment data of the H₂ are taken from ref 4, and the experiment data of C₃H₈ are taken from ref 15.

where $\bar{v} = (8k_B T / \pi m)^{1/2}$ is the average velocity of the thermal motion of the carriers at temperature T , m is the molar mass, and k_B is the Boltzmann constant. The sticking coefficient ϵ measures the destruction efficiency in the collision with the wall, and usually, $\epsilon \approx 10^{-5}$ to 10^{-2} is selected for quartz.⁵ As the reaction vessel used in the Newitt and Thomes experiment is made of transparent silica, the sticking coefficient is taken as 10^{-3} in this study.

3. RESULTS AND DISCUSSION

3.1. Kinetic Model Validation and the Boundary of the Second Explosion Limit. To begin with, the simulation results of the explosion limits for hydrogen and propane with different kinetic mechanisms are presented in Figure 1. Experimental data from Lewis and von Elbe for the hydrogen/oxygen system⁴ and from Newitt and Thomes for the propane/oxygen system¹⁵ are also used to validate these kinetic models. For stoichiometric hydrogen/oxygen, as shown in Figure 1a, all of the kinetic models reproduce the experimentally observed “Z-shaped” explosion limit curve in the pressure and temperature parameter space. The second explosion limit is bounded by two turning points, (P_{1-2} , T_{1-2}) and (P_{2-3} , T_{2-3}). The turning point (P_{1-2} , T_{1-2}) indicates the thermodynamic state that separates the first and second limits, and the point (P_{2-3} , T_{2-3}) indicates the turning from the second limit to the third limit. On the first and the third explosion limit curves, the pressure decreases with an increase of temperature, indicating that at higher temperatures, explosion can be triggered with lower reactant concentrations. On the second explosion limit curve, the pressure increases with an increase of temperature, indicating that the explosion will be triggered with higher reactant concentrations. Additionally, all of the three kinetic models show excellent agreement with the experimental measurement from Lewis, including the prediction of the position and the two turning points that bound the second explosion limit.

The explosion limits for equimolecular propane/oxygen mixture are shown in Figure 1b, and experiments from Newitt and Thomes show that the curve is “S-shaped”. All of the three models qualitatively captured the explosion limit curve, although the turning point predictions deviate slightly from the measurements. Compared with the kinetic models of Aramco 2.0 and KAUST, the methane/propane model shows better agreement between the predicted and measured turning points. Additionally, similar to that of hydrogen, on both the first and third explosion limit curves, the explosion pressure

increases at lower temperatures, and on the second explosion limit curve, pressure increases at higher temperatures. However, the turning point pressure from the first to the second explosion limit P_{1-2} is higher than that from the second to the third explosion limit P_{2-3} , and the turning point temperature T_{1-2} is higher than T_{2-3} , which is different from the hydrogen/oxygen system shown in Figure 1a. This phenomenon is consistent with the negative temperature coefficient (NTC) characteristics for typical hydrocarbons. Because of its good performance for the explosion limit curve prediction, the methane/propane model (C1/C3)²⁴ is then selected for the following calculations of the C0–C3 alkane/oxygen system.

To further verify the prediction ability of the methane/propane mechanism, the comparison between the calculated and experimental explosion limits of methane and ethane are shown in Figure 2. It can be seen that the overall trend of the

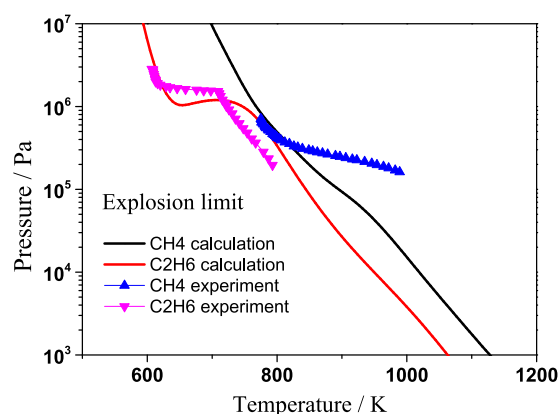


Figure 2. Comparison of the calculated and experimental explosion limits of methane and ethane; the experimental data are taken from ref 25.

calculated results and the experimental results is in good agreement, and the position of the second explosion limit is also very close.

3.2. Second Explosion Limit Dependence on Carbon Number. Since both the first and third explosion limits have been well-recognized and reasonably interpreted by previous investigations,^{6–9} we will then focus on the second explosion limit and see how it changes the Z-curve explosion limit behavior of the hydrogen/oxygen system to the S-curve behavior of the propane/oxygen system by gradually increasing

the carbon number of the fuel. In each calculation, a stoichiometric fuel/O₂ mixture is used.

3.2.1. From C0 to C1. Figure 3 shows the explosion limit curves of the H₂/CH₄/O₂ system with increasing methane

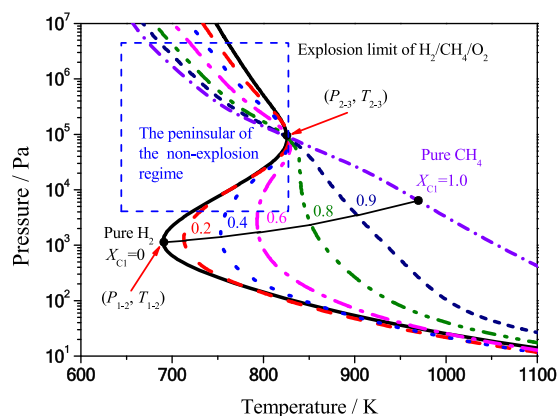


Figure 3. Effect of methane addition on the second explosion limit of hydrogen.

substitution (X_{C1} , the mole fraction of methane in the H₂/methane fuel blends). As can be seen that the upper turning point ($P_{2-3} = 0.86$ bar, $T_{2-3} = 825.8$ K) remains almost unchanged with an increase of CH₄ substitution, indicating that increasing the carbon number has a weak influence on the second to the third explosion limit transition. However, with an increase of X_{C1} , the transition point for the first to the second explosion limit (P_{1-2} , T_{1-2}) gradually moves to the higher-pressure and -temperature region, i.e., (0.012 bar, 712.9 K), (0.014 bar, 753.2 K), and (0.017 bar, 794 K), respectively, for $X_{C1} = 20, 40,$ and 60% . As such, the second limit rotates counterclockwise around the upper turning point and the explosion region is narrowed. In addition, with an increase of X_{C1} , the positive slope of the second explosion limit curve significantly increases to an infinitely large value at $X_{C1} \approx 20\%$. Then, the slope (k_{PT} , defined in Section 3.3) transits to a negative value and the magnitude of the slope decreases with further increasing X_{C1} . As a consequence, the explosion curve transits from nonmonotonic (pure H₂) to monotonic (pure CH₄), and the turning point that separates the three explosion limits cannot be determined clearly such that the second explosion limit vanishes. In this case, we define a pseudo- (P_{1-2}, T_{1-2}) for a higher X_{C1} (>0.8) system by extrapolating the well-defined turning point (P_{1-2}, T_{1-2}) for a lower X_{C1} ($0-0.6$) system to higher X_{C1} cases. In this way, we can clearly see the trend of the second limit behavior, which can be quantified by the value of k_{PT} .

3.2.2. From C1 to C2. Figure 4 shows the explosion limit curves of the CH₄/C₂H₆/O₂ system with increasing ethane substitution (X_{C2} , the mole fraction of methane in the CH₄/C₂H₆ fuel blends). For the methane/oxygen system, the explosion pressure exhibits a monotonic decrease with an increase of temperature in the whole examined region. For $X_{C2} < 10\%$, no obvious turning points show up on the whole explosion limit curve, and with an increase of X_{C2} , the explosion pressure for temperatures higher than 700 K does not change much, while for lower temperatures, the explosion pressure decreases. For $X_{C2} > 10\%$, the increased carbon number results in the presence of two turning points and bound a period of an almost horizontal line. As such, the

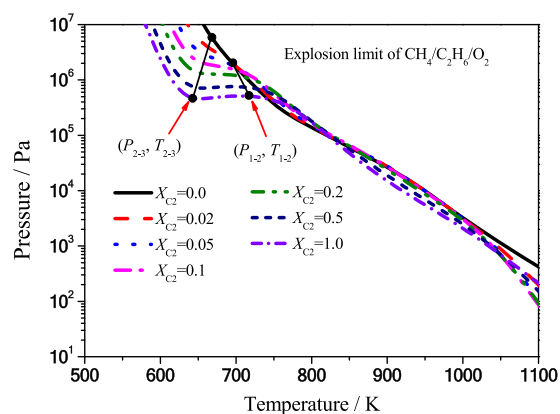


Figure 4. Effect of ethane addition on the second explosion limit of methane.

second explosion limit is retrieved. On the second explosion limit curve, the pressures for different X_{C2} systems all show weak dependence on temperature. However, the turning point for the first to the second limit (P_{1-2} , T_{1-2}) gradually moves to higher temperatures, while the turning point for the second to the third limit transition (P_{2-3} , T_{2-3}) moves to a lower-temperature region, resulting in an expanded second limit region. Because for X_{C2} larger than 10% the two turning points can be well defined, we also extrapolate the bound pressure and temperature on the second explosion limit to lower X_{C2} cases such that we also get two pseudoturning points for lower X_{C2} cases. It is noted that for the pure CH₄/O₂ system ($X_{C1} = 1$ for H₂/CH₄ or $X_{C2} = 0$ for CH₄/C₂H₆ fuel blends), there is no second explosion limit. As such, the pseudoturning points obtained by extrapolating X_{C2} from 1 to 0 in CH₄/C₂H₆ in Figure 4 do not show the pseudoturning points in Figure 3, which is obtained by extrapolating X_{C1} from 0 to 1. It seems that the second limit curve also rotates counterclockwise with an increase of carbon number X_{C2} .

3.2.3. From C2 to C3. Figure 5 shows the explosion limit curves of the C₂H₆/C₃H₈/O₂ system with increasing propane

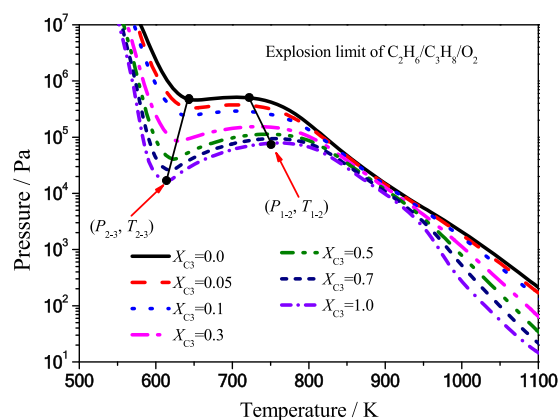


Figure 5. Effect of propane addition on the second explosion limit of ethane.

substitution (X_{C3} , the mole fraction of propane in the C₂H₆/C₃H₈ fuel blends). It is seen that for all different X_{C3} cases, the explosion limit curve is “S”-shaped, and with an increase of X_{C3} , nonmonotonic S-shaped behavior of the curve becomes more severe and the second explosion limit shifts to lower pressures. In addition, the transition point temperature T_{1-2}

gradually moves to a higher-temperature region, while the transition point temperature for the second to the third explosion limit T_{2-3} gradually moves to a lower-temperature region, indicating an extended second explosion limit. Furthermore, the reduction extent of P_{2-3} is comparable to that of P_{1-2} for small X_{C_3} cases, and a more obvious decrease of P_{2-3} is observed when X_{C_3} is larger than 0.1. From ethane to propane, it seems that the second limit curve again rotates counterclockwise with an increase of carbon number X_{C_3} .

3.2.4. Overall Trend of the Second Limit Slope Versus Carbon Number. With an increase of carbon number, the second explosion limit curves all rotate counterclockwise, as shown in Figures 3–5. To more clearly present the effect of carbon number on the second explosion limit, the slope of the quasi-linear relationship between the logarithmic pressure and temperature is derived, as in eq 2.

$$k_{PT} = \frac{(\lg(P_{1-2}/1 \text{ atom}) - \lg(P_{2-3}/1 \text{ atom}))}{(T_{1-2} - T_{2-3})} \quad (2)$$

where P_{1-2} and P_{2-3} are the pressures of the turning points and T_{1-2} and T_{2-3} are the temperatures of the turning points.

Figure 6 shows the k_{PT} as a function of the carbon number. Carbon number ranges of $[0, 1]$, $[1, 2]$, and $[2, 3]$,

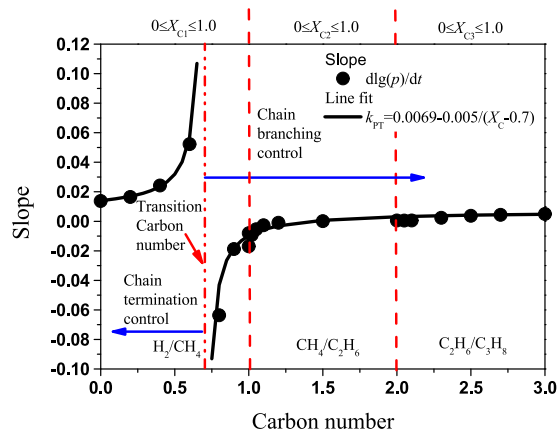


Figure 6. Trends of the slopes of the second explosion limit from C_0 to C_3 .

respectively, represent fuel mixtures of H_2/CH_4 ($0 \leq X_{C_1} \leq 1.0$), CH_4/C_2H_6 ($0 \leq X_{C_2} \leq 1.0$), and C_2H_6/C_3H_8 ($0 \leq X_{C_3} \leq 1.0$).

It is seen that with an increase of carbon number, the slope variations can be divided into two regions. Pure hydrogen has a positive slope, further increasing X_{C_1} initially weakly and then significantly increasing the slope to an infinitely large value at $X_{C_1} \approx 0.7$ (carbon number ≈ 0.7). Then, the slope just changes from positive infinity to negative infinity and the magnitude gradually decreases. As the carbon number further increases, the slope magnitude gradually decreases to zero at the carbon number around 1.5 ($X_{C_2} \approx 0.5$). Further increasing the carbon number only weakly increases the slope with a positive sign. The dependence of the slope of the second explosion limit on the carbon number can be expressed as the following function

$$k_{PT} = 0.0069 - 0.005/(X_c - 0.7) \quad (3)$$

It is shown from Figure 6 that the slope calculated by this fit function agrees well with the slope calculated from the

explosion limit curve. Therefore, the slope of the second explosion limit is inversely proportional to the carbon number.

3.3. Controlling Elementary Reactions for the Second Explosion Limit. We note that the second explosion limit is controlled by the competition between the chain branching and termination reactions.^{4,11} For the carbon number lower than 0.70, chain termination reactions dominate the second explosion limit because the transition temperature T_{2-3} is larger than T_{1-2} , resulting in a nonexplosion peninsula, as shown in Figure 3. With an increase of carbon number, T_{1-2} gradually increases and approaches T_{2-3} . As such, the nonexplosive peninsula gradually narrows, indicating that the chain termination reactions become weaker compared to the chain branching reactions. When the carbon number is increased to around 0.70, T_{1-2} equals T_{2-3} , the nonexplosive peninsula vanishes, and the roles of the chain termination reactions and the chain branching reactions are comparable. For the carbon number higher than 0.70, T_{1-2} is always larger than T_{2-3} , indicating that the chain branching reactions become dominant in controlling the second explosion limit. Additionally, since the kinetics of different fuel systems inherently contain different chain termination and chain branching reactions, we will then examine further what are those elementary reactions (either chain branching or termination) that dominate the second explosion limit.

To realize this goal, a two-step approach is adopted. First, to find the key reactions controlling the second explosion limit behavior for C_0 – C_3 alkane molecules, the sensitivity analysis is conducted by perturbing the rate constant of each elementary reaction and comparing the corresponding explosion limit curve with the original one. In each sensitivity calculation, the pre-exponential factor of the rate constant is reduced by 90% for each individual reaction. The explosion limit curve calculated by the modified mechanism will be compared with that calculated by the original mechanism. The reactions that have an obvious effect on the explosion curves will be retained in the reduced mechanism. As the key reactions related to the explosion limit of pure hydrogen have been studied extensively in previous research, the sensitivity analysis with respect to hydrogen is not performed in this study.^{12,14} Instead, a nine-reaction mechanism is directly used as the reduced mechanism of hydrogen, where the reaction rate constants and the thermal parameters are all taken from the methane/propane model.²⁴

The sensitivity analysis shows that a total number of 30 reactions should be retained to reproduce the explosion limit of methane calculated by the detailed mechanism. In addition, the explosion limit of C_2H_6 can be well reproduced with 77 reactions based on the sensitivity analysis. Furthermore, to maintain the accuracy of the explosion limit calculations, a total number of 194 reactions are kept in the reduced mechanism for C_3H_8 . The explosion limits of the stoichiometric hydrogen/oxygen, methane/oxygen, ethane/oxygen, and propane/oxygen mixtures calculated by the detailed and reduced mechanisms are compared in Figure 7. It is shown that the shape and position of the explosion limits calculated by the detailed mechanism can be well reproduced by the reduced mechanisms with 9, 30, 77, and 194 reactions for hydrogen, methane, ethane, and propane, respectively.

Second, we remove the most sensitive elementary reactions in the reduced mechanism one at a time and compare the correspondingly calculated second explosion limit with the original reduced model. By doing this, the elementary reactions

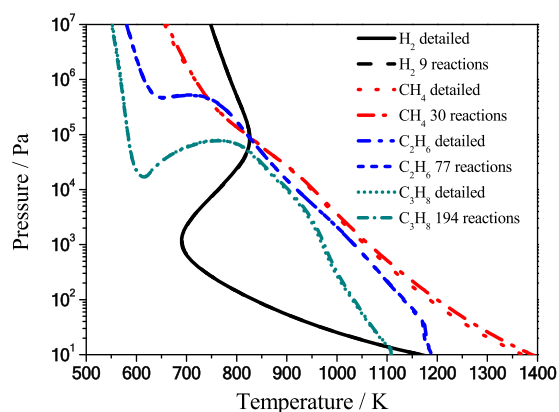


Figure 7. Comparison of the calculation explosion limits of H_2 , CH_4 , C_2H_6 , and C_3H_8 with the detailed and reduced mechanism.

that affect the second explosion limit most will be found out. The criterion is to see whether the complete explosion limit curve will lose its nonmonotonic behavior for hydrogen, ethane, or propane. In the following, we apply these two steps toward hydrogen, methane, ethane, and propane systems, respectively.

3.3.1. Toward H_2 and CH_4 . We first compare the explosion limit curves calculated by the reduced mechanism (black solid line) and the mechanism with reducing the rate constant of $H + O_2 \rightleftharpoons O + OH$ (red dash) and $H + O_2 + M \rightleftharpoons HO_2 + M$ (blue dot) by 90%, as shown in Figure 8a. Other elementary reactions that have much weaker effects are not shown. This comparison indicates that the third-body termination reaction $H + O_2 + M \rightleftharpoons HO_2 + M$ and the chain branching reaction $H + O_2 \rightleftharpoons O + H$ are the most sensitive in determining the explosion limit for hydrogen. For methane, as shown in Figure 8b, the explosion limit curve is monotonic and these two reactions have almost no effect on the explosion limit curve.

For the second step, the explosion limits of hydrogen and methane are calculated without including the termination reaction ($H + O_2 + M \rightleftharpoons HO_2 + M$) or the branching reaction ($H + O_2 \rightleftharpoons O + OH$) in the reduced mechanisms, as shown in Figure 9. It is obvious that the explosion limit curve of hydrogen will lose its nonmonotonic characteristics when the termination reaction is excluded in the reduced mechanisms and the reactivity of the system is significantly improved, as shown in Figure 9a. In addition, when the branching reaction is not included in the reaction mechanism, the reactivity of the hydrogen/oxygen mixture reduces significantly as the explosion limit moves toward a high-temperature region.

However, there is only a very small shift for the methane explosion limit without including the termination or branching reaction in the reduced mechanism, as shown in Figure 9b. So, the dominated chemical kinetics of these two fuels on the explosion limit is inconsistent.

The main reactions with larger sensitivity on the explosion limit of methane are given in Figure 10. The oxidation of methane is initiated by $CH_4 + O_2 = CH_3 + HO_2$, from which the methyl and OH radicals will be generated. After the radical pool is formed, the most sensitive methane-related reactions are $CH_4 + OH \rightleftharpoons CH_3 + H_2O$ and $CH_4 + HO_2 \rightleftharpoons CH_3 + H_2O_2$. The reaction of methyl (CH_3) with hydroperoxyl (HO_2) is important as the concentrations of both radicals are very high during the oxidation process of methane. The reaction path can be a chain-propagating reaction $CH_3 + HO_2 = CH_3O + OH$ or a termination reaction $CH_3 + HO_2 = CH_4 + O_2$. The reaction of the formyl radical is considered important for flame speed predictions. For explosion limit calculations, the formyl decomposition reaction $HCO + M = H + CO + M$ and the reaction with molecular oxygen $HCO + O_2 = CO + HO_2$ are both important. The formyl radical is generated from CH_2O reacted with OH and CH_3 . Also, CH_2O radicals are produced from CH_3 and CH_3O in their reaction with molecular oxygen. The reactions involving methyl, methoxy, and methylperoxy have a significant effect on the explosion limit of methane. This means that for the methane oxidation process the reactive free radicals are mainly generated through the C_1 subset reactions, which are very important in reproducing the correct kinetic behavior. As the explosion limit was no longer dominated by the chain termination reaction, the explosion limit has no nonmonotonic characteristics compared with the explosion limit of hydrogen.

3.3.2. Toward C_2H_6 . By the same approach, we have first found the seven elementary reactions exhibiting the largest sensitivity with respect to the explosion limit of C_2H_6 , as shown in Figure 11. Similar to the methane case, the branching reaction $H + O_2 \rightleftharpoons O + H$ also has almost no effect on the explosion limit. However, the H_2O_2 decomposition reaction obviously affects the first explosion limit. We note that after the radical pool is formed, ethane is mainly consumed through H-abstraction by H or HO_2 , instead of by O_2 . The ethylperoxy radical $C_2H_5O_2$ is largely produced by the addition of molecular oxygen to the ethyl radical due to the long lifetime of RO_2^* radicals, which is the most important species for ethane oxidation.²⁶ The ethylperoxy radical can further abstract a hydrogen atom from ethane to generate $C_2H_5O_2H$ through $C_2H_6 + C_2H_5O_2 \rightleftharpoons C_2H_5 + C_2H_5O_2H$. The cleavage

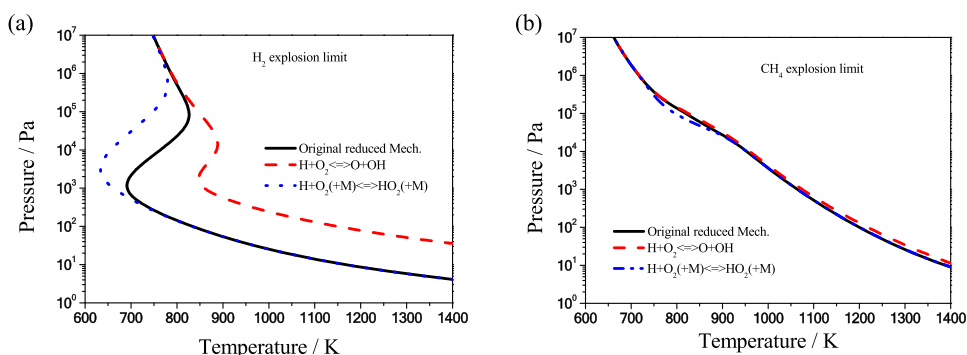


Figure 8. Sensitivities of the chain termination and branching reactions on the explosion limits of hydrogen (a) and methane (b).

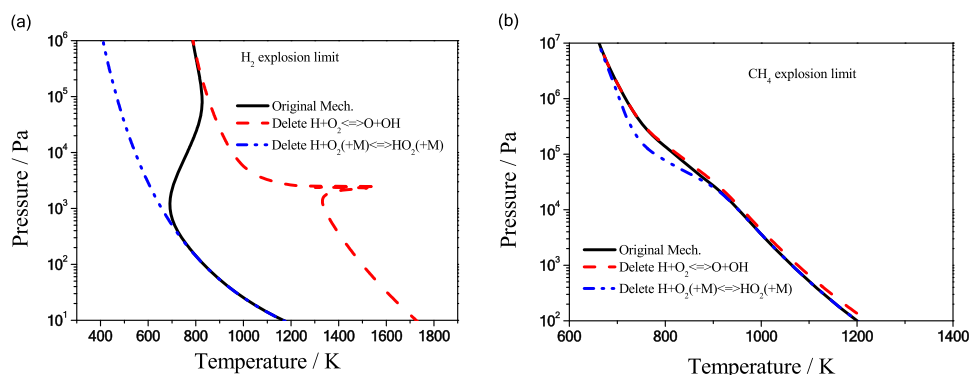


Figure 9. Effect of the chain and termination reaction on the second explosion limits of hydrogen (a) and methane (b).

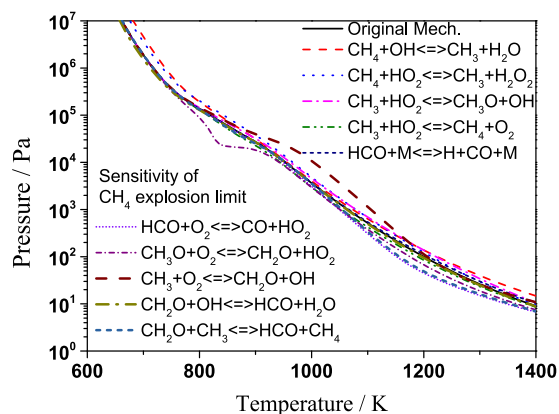


Figure 10. Main reactions with larger sensitivity on the explosion limit of methane.

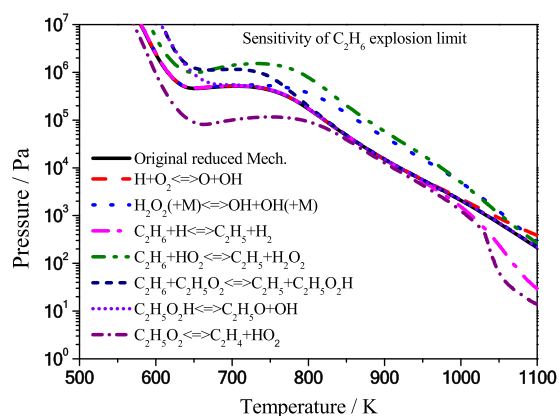


Figure 11. Reactions exhibiting the largest sensitivities with respect to the explosion limit of C₂H₆.

of the weak O–O bond of C₂H₅O₂H leads to a chain branching reaction C₂H₅O₂H ⇌ C₂H₅O + OH.²⁷ As the rate of the C₂H₅O₂H generation reaction reduces, the length of the second explosion limit reduces and P_{1–2} and P_{2–3} both increase. The reduction of the reaction rate of C₂H₅O₂H ⇌ C₂H₅O + OH will shorten the length of the second explosion limit, while P_{1–2} is almost not changed. Under low-pressure conditions, C₂H₅O₂H is largely decomposed to C₂H₄ + HO₂. With the reduction of the rate of C₂H₅O₂H decomposition, both P_{1–2} and P_{2–3} are reduced obviously. For the ethane system, the hydroperoxyethyl species C₂H₄O₂H is unimportant

for the explosion limit of ethane because only a negligibly small amount of C₂H₅O₂ undergoes the isomerization process.²⁶

Figure 12 shows that when C₂H₅O₂H ⇌ C₂H₅O + OH is removed in the mechanism, the calculated explosion limit

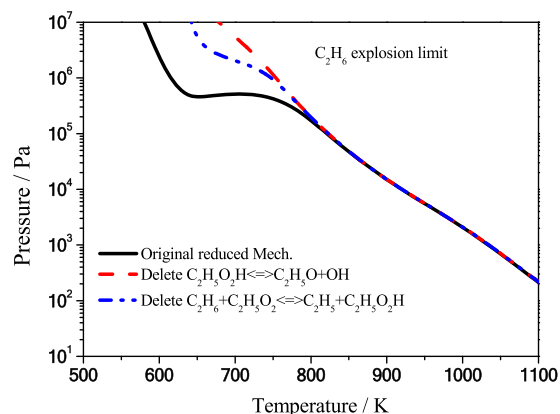


Figure 12. Dominant reactions for the explosion limit behaviors of C₂H₆.

changes drastically and becomes monotonic. In addition, removing C₂H₆ + C₂H₅O₂ ⇌ C₂H₅ + C₂H₅O₂H will significantly shorten the length of the second explosion limit and the second limit is shifted to higher pressures. The C₂H₅O₂H decomposition to form the OH radical is dominant in controlling the nonmonotonic behavior of the second explosion limit of C₂H₆.

3.3.3. Toward C₃H₈. As the carbon number increases, more reaction channels become to affect the explosion limit curve,²⁸ and the determination of the dominant reaction for the second explosion limit of C₃H₈ is more complex since more fuel-specific reactions are affecting the explosion limit behavior. Figure 13 shows that the most sensitive reactions do not affect the general nonmonotonic explosion limit behavior but only shift the two turning points. H-abstraction from propane by OH and HO₂ produces two isomers. *n*-Propyl (*n*-C₃H₇) and *iso*-propyl (*i*-C₃H₇) are generated by OH,²⁹ and *i*-C₃H₇ is produced through hydrogen abstraction by the HO₂ radical. Then, the addition of produced propyl radicals to molecular oxygen forms propylperoxy radicals (C₃H₇O₂), which then undergo the isomerization process to generate the propylhydroperoxy radical C₃H₆OOH. The propylhydroperoxy radical can decompose to C₃H₆ + HO₂ or react with molecular oxygen to form C₃H₆OOHO₂. The formed C₃H₆OOHO₂ will decompose to c3ket + OH. Thereafter, the decomposition of

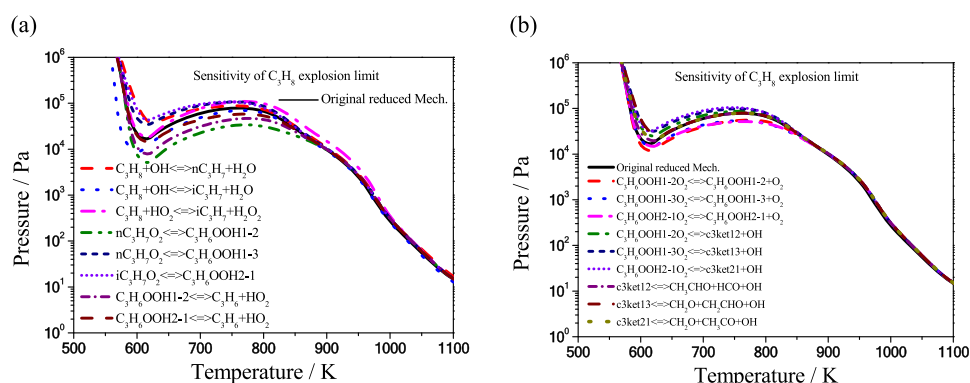


Figure 13. Most sensitive reactions and their effect on the explosion limit behaviors of C_3H_8 (a, b).

c3ket will generate a second OH radical. These reactions have also been recognized to be responsible for the NTC behavior of the larger hydrocarbons.³⁰

Figure 14 further shows the comparison between the calculated explosion limits with removing the three types of

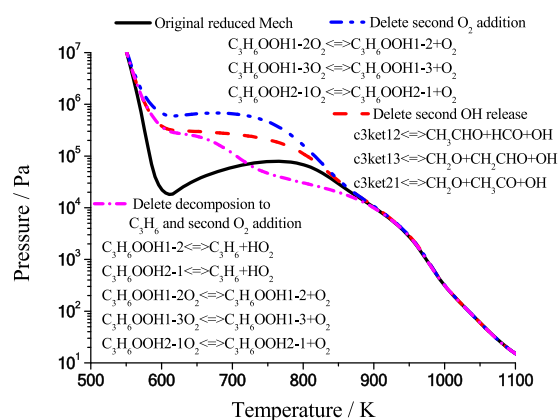


Figure 14. Dominant reactions for the second explosion limit of C_3H_8 .

reaction groups and the calculations with the original mechanism. First, if the reaction path of the molecular oxygen addition to propylhydroperoxyl radical (the second O_2 addition) is cut off, which is used to block the formation of the twice OH radical generation in the chain branching path, the second explosion limit changes to almost a horizontal line instead of the nonmonotonic curve. Second, the second explosion limit still appears as a line with a small inclined angle when the second OH release reactions (the c3ket decomposition reactions) are deleted from the mechanism. This is because the first OH release reactions are still working. Third, when the reactions of the molecular oxygen addition and the decomposition of C_3H_6OOH are both excluded from the mechanism, a quasi-monotonic explosion limit curve is achieved. This means that C_3H_6OOH undergoes the decomposition reaction when the molecular oxygen addition reaction path is blocked, which will generate the C_3H_6 radical. The C_3H_6 subset reactions will give an explosion limit similar to that of C_2H_6 . From the above analysis, it is concluded that the second explosion limit behavior of propane is governed by the three sets of reactions, as presented in Figure 14.

4. CONCLUSIONS

In this study, the explosion limits of the typical C_0 – C_3 alkanes are analyzed computationally and theoretically. The critical path of the reaction influencing the second explosion limit is found. The key elementary reactions affecting the explosion limit of C_0 – C_3 alkanes are obtained.

The second explosion limit of pure hydrogen has a positive slope, further increasing X_{C1} initially weakly then significantly increases the slope to an infinitely large value at $X_{C1} \approx 0.7$. Then, the slope just changes from positive infinity to negative infinity and the magnitude gradually decreases. As the carbon number further increases, the slope magnitude gradually decreases to zero at the carbon number around 1.5. Further increasing the carbon number only weakly increases the slope with a positive sign. The dependence of the slope of the second explosion limit on the carbon number can be expressed using an inverse proportional function.

The termination reaction $H + O_2 + M \rightleftharpoons HO_2 + M$ and the chain branching reaction $H + O_2 \rightleftharpoons O + H$, which are the key reactions in determining the explosion limit of C_0 , have a very small effect on the explosion limit of $C1$ – $C3$. The non-monotonic characteristic of the $C2$ explosion limit is controlled by the chain propagation reaction $C_2H_5O_2H \rightleftharpoons C_2H_5O + OH$. The NTC behavior in the explosion limit of $C3$ is governed by the low-temperature reactions of C_3H_8 , which will generate two OH radicals and significantly improve the reactivity of the system.

AUTHOR INFORMATION

Corresponding Authors

Jie Liu – Department of Power Mechanical Engineering, Beijing Jiaotong University, Beijing 100044, P. R. China; orcid.org/0000-0002-0243-9127; Phone: +0086 10 51684279; Email: ljie@bjtu.edu.cn

Chenglong Tang – School of Energy and Power Engineering, Xi'an Jiaotong University, Xi'an 710049, P. R. China; Email: chenglongtang@mail.xjtu.edu.cn

Authors

Ruiguang Yu – Department of Power Mechanical Engineering, Beijing Jiaotong University, Beijing 100044, P. R. China

Biao Ma – Department of Power Mechanical Engineering, Beijing Jiaotong University, Beijing 100044, P. R. China

Complete contact information is available at: <https://pubs.acs.org/10.1021/acsomega.0c02825>

Notes

The authors declare no competing financial interest.

ACKNOWLEDGMENTS

This study is supported by the International Science and Technology Cooperation of China (No. 2019YFE0100200) and the National Natural Science Foundation of China (No. 51406007). The authors gratefully acknowledge the valuable discussion with Prof. John Griffiths from the University of Leeds.

REFERENCES

- (1) Su, B.; Luo, Z.; Wang, T.; Yan, K.; Cheng, F.; Deng, J. Coupling Analysis of the Flame Emission Spectra and Explosion Characteristics of CH₄/C₂H₆/Air Mixtures. *Energy Fuels* **2020**, *34*, 920–928.
- (2) Ajrash, M. J.; Zanganeh, J.; Moghtaderi, B. Influences of the Initial Ignition Energy on Methane Explosion in a Flame Deflagration Tube. *Energy Fuels* **2017**, *31*, 6422–6434.
- (3) Huang, L.; Wang, Y.; Yang, Z.; Wang, Q.; Pei, S.; Zhang, L.; Ren, S. Flammability and Explosion Characteristics of Methane in Oxygen-Reduced Air and Its Application in Air Injection IOR Process. *Energy Fuels* **2019**, *33*, 11850–11860.
- (4) Lewis, B.; von Elbe, G. *Combustion; Flames; and Explosions of Gases*, 2nd ed.; Academic Press: New York, 1961.
- (5) Wang, X.; Law, C. K. An analysis of the explosion limits of hydrogen-oxygen mixtures. *J. Chem. Phys.* **2013**, *138*, No. 134305.
- (6) Semenov, N. N. *Some Problems in Chemical Kinetics and Reactivity*; Princeton University: New Jersey, 1959.
- (7) Glassman, I.; Yetter, R. A. *Combustion*, 4th ed.; Elsevier: New York, 2008.
- (8) Azatyan, A. A.; Andrianova, Z. S.; Ivanova, A. N. Role of the HO₂ radical in hydrogen oxidation at the third self-ignition limit. *Kinet. Catal.* **2010**, *51*, 337–347.
- (9) Sánchez, A. L.; Fernández-Tarrazo, E.; Williams, F. A. The chemistry involved in the third explosion limit of H₂–O₂ mixtures. *Combust. Flame* **2014**, *161*, 111–117.
- (10) Law, C. K. *Combustion Physics*; Cambridge University Press, 2006.
- (11) Sher, E.; Sher, I.; Bar-Kohany, T. Another view of the upper and intermediate explosion limits of H₂-O₂ system. *Int. J. Hydrogen Energy* **2013**, *38*, 14912–14914.
- (12) Liang, W.; Liu, J.; Law, C. K. On explosion limits of H₂/CO/O₂ mixtures. *Combust. Flame* **2017**, *179*, 130–137.
- (13) Liang, W.; Liu, Z.; Law, C. K. Explosion limits of H₂/CH₄/O₂ mixtures: Analyticity and dominant kinetics. *Proc. Combust. Inst.* **2018**, *37*, 1–8.
- (14) Liu, J.; Wang, J.; Zhang, N.; et al. On the explosion limit of syngas with CO₂ and H₂O additions. *Int. J. Hydrogen Energy* **2018**, *43*, 3317–3329.
- (15) Newitt, D. M.; Thornes, L. S. The Oxidation of Propane. Part I. The Products of the Slow Oxidation at Atmospheric and at Reduced Pressures. *J. Chem. Soc.* **1937**, 1656–1665.
- (16) Wang, Z.; Gou, X.; Zhong, C. Experimental and Kinetic Study on the Cool Flame Characteristics of Dimethyl Ether. *Energy Fuels* **2019**, *33*, 9205–9214.
- (17) Liu, C.; Zhang, Y.; Xiong, D.; et al. Flammability and Propagation Dynamics of Planar Freely Propagating Dimethyl Ether Premixed Flame. *ACS Omega* **2020**, *5*, 10965–10976.
- (18) Yu, R.; Liu, J.; Ma, B. The dependence of NTC behavior on the equivalence ratio and nitrogen fraction in cool flame region. *Fuel* **2020**, *271*, No. 117623.
- (19) Liu, Jie.; Yu, R.; Ma, B. Effect of Ozone Addition on the Cool Flame and Negative Temperature Coefficient Regions of Propane-Oxygen Mixtures. *ACS Omega* **2020**, *5*, 16448–16454.
- (20) Lutz, A. E.; Kee, R. J.; Miller, J. A. *SENKIN: A FORTRAN Program For Predicting Homogeneous Gas Phase Chemical Kinetics with Sensitivity Analysis*, No. SAND-87-8248; Sandia National Laboratories: Livermore, CA, 1988; 87–8248.
- (21) Guo, J.; Peng, W.; Zhang, S.; Lei, J.; Jing, J.; Xiao, R.; Tang, S. Comprehensive Comparison of the Combustion Behavior for Low-Temperature Combustion of n-Nonane. *ACS Omega* **2020**, *5*, 4924–4936.
- (22) Atef, N.; Kukkadapu, G.; Mohamed, S. Y.; et al. A comprehensive iso-octane combustion model with improved thermochemistry and chemical kinetics. *Combust. Flame* **2017**, *178*, 111–134.
- (23) Li, Y.; Zhou, C. W.; Somers, K. P.; et al. The Oxidation of 2-Butene: A High Pressure Ignition Delay, Kinetic Modeling Study and Reactivity Comparison with Isobutene and 1-Butene. *Proc. Combust. Inst.* **2017**, *36*, 403–411.
- (24) Petersen, E. L.; Kalitan, D. M.; Simmons, S.; et al. Methane/Propane Oxidation at High Pressures: Experimental and Detailed Chemical Kinetic Modelling. *Proc. Combust. Inst.* **2007**, *31*, 447–454.
- (25) Townend, D. T. A.; Chamberlain, E. A. C. The influence of pressure on the spontaneous ignition of inflammable gas-air mixtures – IV-methane-, ethane-, and propane-air mixtures. *Proc. R. Soc. London, Ser. A* **1936**, *154*, 95–112.
- (26) Hashemi, H.; Jacobsen, J. G.; Rasmussen, C. T.; et al. High-pressure oxidation of ethane. *Combust. Flame* **2017**, *182*, 150–166.
- (27) Naik, C. V.; Dean, A. M. Detailed kinetic modeling of ethane oxidation. *Combust. Flame* **2006**, *145*, 16–37.
- (28) Bai, S.; Davis, M. J.; Sivaramakrishnan, R.; et al. A chemical pathway perspective on the kinetics of low-temperature ignition of propane. *Combust. Flame* **2019**, *202*, 154–178.
- (29) Hashemi, H.; Christensen, J. M.; Harding, L. B.; et al. High-pressure oxidation of propane. *Proc. Combust. Inst.* **2019**, *37*, 461–468.
- (30) Ji, W.; Zhao, P.; He, T.; et al. On the controlling mechanism of the upper turnover states in the NTC regime. *Combust. Flame* **2016**, *164*, 294–302.